Research Article | Vol. 27, No. 1 | 7 Jan 2019 | OPTICS EXPRESS 175

Optics EXPRESS

Programmable pulse shaping for time-gated amplifiers

J. PUPEIKIS,* N. BIGLER, S. HRISAFOV, C. R. PHILLIPS, AND U. KELLER

Department of Physics, Institute for Quantum Electronics, ETH Zurich, August-Piccard-Hof 1 8093 Zurich, Switzerland
pupeikis@phys.ethz.ch

Abstract: We experimentally demonstrate a novel use of a spatial light modulator (SLM) for shaping ultrashort pulses in time-gated amplification systems. We show that spectral aberrations because of the device's pixelated nature can be avoided by introducing a group delay offset to the pulse via the SLM, followed by a time-gated amplification. Because of phase wrapping, a large delay offset yields a nearly-periodic grating-like phase function (or a phase grating). We show that, in this regime, the phase grating periocidity defines the group delay spectrum applied to the pulse, while the grating's amplitude defines the fraction of light that is delayed. We therefore demonstrate that a one-dimensional (1D) SLM pixel array is sufficient to control both the spectral amplitude and the phase of the amplified pulses.

© 2019 Optical Society of America under the terms of the OSA Open Access Publishing Agreement

1. Introduction

Femtosecond pulse shaping is nowadays an integral part of ultrafast optics technology. Pulse shaper applications are extremely broad and include time-resolved spectroscopy, laser-matter interaction experiments, metrology, machining of materials, optical communication and many others [1]. In complex high-power laser systems, the pulse shapers are typically an integral part of the front-end of the systems and play a major role in managing dispersion [2–4].

Spatial light modulator (SLM) based pulse shapers are ubiquitous, despite the fact that the pixelated nature of the device leads to various kind of waveform aberrations [5]. The discrete phase sampling nature and the presence of gaps between the pixels leads to a time-domain comb of sampling replica pulses. Furthermore, another class of waveform distortion appears when a large phase is applied. Because SLM-based pulse shapers are usually capable of applying only up to 2π radians of phase, the effective large phase is applied by phase wrapping, i.e. $\varphi_{wrapped} = \mathrm{mod}(\varphi_{ideal,}\ 2\pi)$. Phase wrapping leads to abrupt phase jumps, which some SLMs cannot exactly reproduce due to pixel crosstalk or limited spectral resolution. In the presence of such crosstalk, wrapping causes the phase to smoothly evolve from 2π to 0 over a finite region of the SLM, as illustrated in Fig. 1(a). This transition corresponds to a phase error and introduces aberrations on the shaped pulse. If a large phase slope versus frequency is applied, the wrapped phase can effectively be considered as a periodic phase grating in the frequency domain. In time-domain this leads to an appearance of a series of "diffraction" orders, known as modulator replicas [5].

Which kind of waveform distortions dominate depends strongly on the type of the SLM pulse shaper design. Liquid crystal (LC) SLMs typically have a low number of pixels separated by large gaps leading to significant sampling replicas and weaker modulator replicas, as it was well studied in [5]. On the other hand, liquid crystal on silicon (LCoS) SLMs have smaller gaps leading to a relatively strong inter-pixel coupling [6]. Because of this property, sampling replicas are typically well suppressed while stronger modulator replicas emerge.

Modulator replicas can be avoided using spatial diffraction-based pulse shaping with a 2D-SLM [7]. Although this method additionally allows for amplitude shaping, it requires a 2D pixel array. It has also been demonstrated that a 1D-LCoS SLM can be used for both

#349418 10.1364/OE.27.000175
Journal © 2019 Received 31 Oct 2018; revised 18 Dec 2018; accepted 19 Dec 2018; published 3 Jan 2019
Corrected: 7 June 2020

Optics EXPRESS

phase and amplitude control by oversampling the Fourier plane [8]. However, spectral distortions due to phase wrapping are still present in this technique. An alternative to the SLM-based pulse shaper is an acousto-optic programmable dispersive filter (AOPDF) [9]. AOPDFs are used in chirped pulse amplification (CPA) systems because they do not generate pulse replicas [10], and they can apply a large spectral phase while also controlling the spectral amplitude [11–13]. However, AOPDFs can be operated at a limited repetition rate and diffraction efficiency due to the need to continually generate new acoustic waves to modulate the acousto-optic crystal at the laser repetition rate. Currently, the highest repetition rate AOPDF-controlled system was demonstrated at 100 kHz [13].

In this paper, we experimentally demonstrate an alternative use of a one-dimensional (1D) SLM which allows for a simultaneous amplitude and phase control without spectral interferences from the replica pulses. Our approach applies to time-gated amplifiers, which include optical parametric chirped pulse amplifiers (OPCPAs) [14,15] or frequency-domain optical parametric amplifiers (FOPAs) [16,17]. In these systems amplification only occurs within the temporal duration of the short pump pulse, providing a time-gating effect. Here we show that by adding a large group delay (GD) offset on a phase-only 1D-SLM followed by a time-gated amplification, we can achieve a full amplitude and phase shaping of ultrashort pulses without aberrations or modulator replica pulses.

In section 2 we explain the scheme conceptually, while, in section 3 we demonstrate it experimentally using an OPCPA system. Finally, in section 4 we experimentally and theoretically demonstrate the amplitude shaping capability.

2. Time-gated filtering scheme

The time-gated filtering scheme is conceptually illustrated in Fig. 1, where we sketch a pulse compression scheme using a pulse shaper followed by a time-gated amplifier. As discussed in the introduction, applying a phase larger than 2π radians on a pulse using a pulse shaper can lead to waveform distortions. Because the phase smoothly evolves from 2π to 0 due to crosstalk, as shown in Fig. 1(a), the spectral components around the 2π to 0 transition will experience a different phase than originally applied, which will distort the waveform around the zero-delay. Here we overcome this problem by applying a sufficiently large GD to the SLM, such that the delayed light can avoid these temporal aberrations.

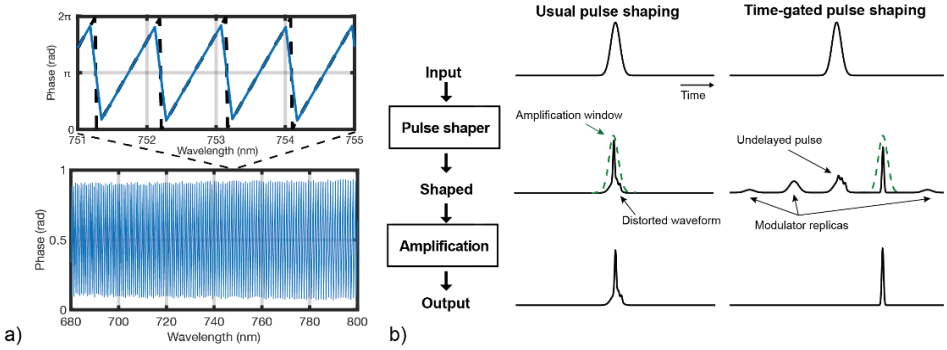

Fig. 1. a) Phase-wrapped group delay (GD) of 2000 fs. For illustrative purposes, the pixel crosstalk was simulated using a moving average filter with a width of 8 pixels. The snippet shows a zoomed in phase where deviation from the ideal wrapped phase (dashed black line) is clearly visible. b) Conceptual illustration of how we can increase the engineered waveform quality by adding a GD on the pulse with the pulse shaper and amplifying the delayed pulse using a time-gated amplifier.

As an example, suppose we wish to impose a spectral phase profile $\varphi_{target}(\omega)$, onto a pulse in order to optimize its compression. Phase wrapping and pixel crosstalk will lead to aberrations, and these aberrations will distort the shaped pulse (see Fig. 1(b), usual pulse shaping). However, by applying a large GD offset, the corresponding ideal phase $\varphi_{ideal}(\omega)$ =

Optics EXPRESS

$\varphi_{target}(\omega)$ + GD·$(\omega-\omega_0)$ will be a nearly-linear function (here ω_0 is the center frequency). The subsequent phase wrapping operation will yield a nearly periodic $\varphi_{wrapped}(\omega)$ phase. This wrapped phase resembles a phase grating in the frequency domain. However, due to the pixel crosstalk, the amplitude of the phase grating $\varphi_{wrapped}(\omega)$ will be reduced and smoothed as we show in Fig. 1(a). This periodic deviation from an ideal linear spectral phase will lead to the appearance of the modulator replicas in the time domain. From the Fourier theory, these replicas are temporally delayed by integer multiples of the applied GD offset, where the GD offset is the inverse of the period in frequency. The modulator replicas are illustrated in Fig. 1(b) ("shaped" waveform). Although the GD offset leads to replicas, the waveform can effectively be cleaned using a temporal filter. For example, a time-gated amplifier can be controlled to only amplify the first replica, which is free of the temporal aberrations appearing around the zero-delay, as shown in Fig. 1(b) ("output" waveform).

3. Experimental setup

Figure 2 shows our experimental implementation. Here we use a part of our already reported OPCPA chain [4,18] and we focus on the pulse shaping aspect in more detail. A reflective liquid crystal on silicon (LCoS) SLM is placed in a Fourier plane of a 4-f pulse shaper setup. The SLM is a one-dimensional array of 12288 pixels (BNS-Linear-12288, Meadowlark Optics Inc.). The pixel dimension is 1 μm horizontally and 19.66 mm vertically with 0.6 μm gaps between the electrodes. The pulse shaper is used to control the spectral phase and amplitude of a Ti:sapphire oscillator output (Venteon Pulse: One < 6 fs, Laser Quantum Ltd.) operating at a repetition rate of 82 MHz. To increase the spectral resolution of the Fourier plane and thereby leverage the large number of pixels available, we expanded the Ti:sapphire output beam in the horizontal axis to obtain a radius of 1.4 mm ($1/e^2$) while the vertical axis has a radius of 0.7 mm before entering the pulse shaper. The beam is spectrally dispersed using a reflection grating with 600 grooves/mm (10RG600-800-1, Newport Corp.) and spectrally focused in the horizontal axis on the SLM with a cylindrically curved mirror of 100 mm focal length. The SLM is slightly vertically tilted so that the returning beam is reflected with a D-shaped mirror.

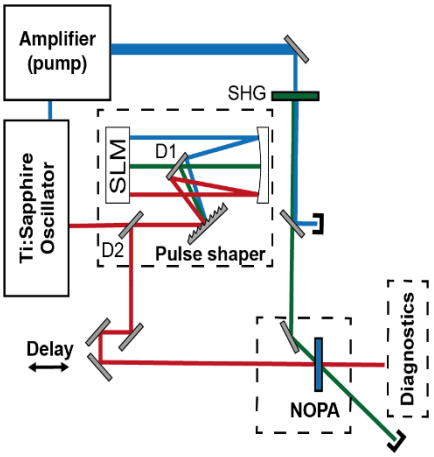

Fig. 2. Our experimental setup. A reflective 4-f pulse shaper is used to control the phase of the seed for a non-collinear optical parametric amplifier (NOPA). The geometry of the pulse shaper setup (dashed box) is as follows. The incident beam is first reflected from the diffraction grating, then a D-shaped mirror (D1) directs the angularly chirped beam towards the cylindrical mirror. The cylindrical mirror is tilted upwards so that the reflected light reaches the spatial light modulator (SLM). The SLM is tilted downwards so that the returning beam is reflected by a second D-shaped mirror (D2). For time-gated amplification, a narrow-band pump pulse (wavelength 1030 nm) is frequency doubled in a second harmonic generation (SHG) stage and is used to amplify the seed in the NOPA.

Optics EXPRESS

Part of the Ti:sapphire oscillator bandwidth around 1030 nm is used to seed an Yb:YAG based amplifier chain (A400, Amphos GmbH) which yields high-power 1.8 ps pulses at 100 kHz. A fraction of the amplifier output power is frequency doubled, and this 515-nm pump beam is used to amplify the shaped Ti:sapphire pulses in a non-collinear optical parametric amplifier (NOPA). In this paper we use the NOPA to perform a time-frequency analysis of the shaped near-IR pulses by varying the pump-signal delay. The NOPA, which is operated in a non-saturated regime, is based on a 1.8-mm-thick BBO crystal configured for type-I phase-matching. We characterize the amplified signal pulses with a spectrometer and a second harmonic frequency resolved optical gating (SH-FROG) [19]. Because the NOPA was optimized for generating the mid-infrared seed pulses for the above-mentioned OPCPA chain, only spectral components between 650 and 800 nm are amplified. However, the implemented pulse shaper supports a larger bandwidth of 640-930 nm.

The pulse shaper acts as a main dispersion control element for our OPCPA system. Such OPCPA systems usually require a relatively large phase tuning range. For example, to compensate for a third-order dispersion (TOD) of 50000 fs^3 over the 650-800 nm spectral range for a central wavelength of 745 nm, 160 radians of phase need to be applied as it is illustrated in Fig. 3(a). However, as explained in section 2, this requires phase wrapping and leads to modulator replica pulses and corresponding spectral interferences. To illustrate this issue, in Fig. 3(c) we show the NOPA amplified spectrum versus delay between the pump and the seed for an example configuration. Positive delay values correspond to the pump pulses arriving after the seed pulses. In the example shown, we have applied −50000 fs^3 TOD at a central wavelength of 745 nm. From the Fig. 3(c), it can be clearly seen that some spectral components are temporally spread out around the main pulse. Figure 3(a) shows the phase profile which we wrapped and sent to the SLM device. The rapid change in phase derivative due to phase wrapping corresponds to the spread-out temporal features in the measurement. These waveform distortions can be attributed to the smoothed phase wrapping due to pixel crosstalk as discussed in section 2. We validated this by simulating the influence of a wrapped and smoothed spectral phase profile (Fig. 3(b)) by performing a time-frequency analysis on a simulated time-domain representation of the waveform (Fig. 3(d)).

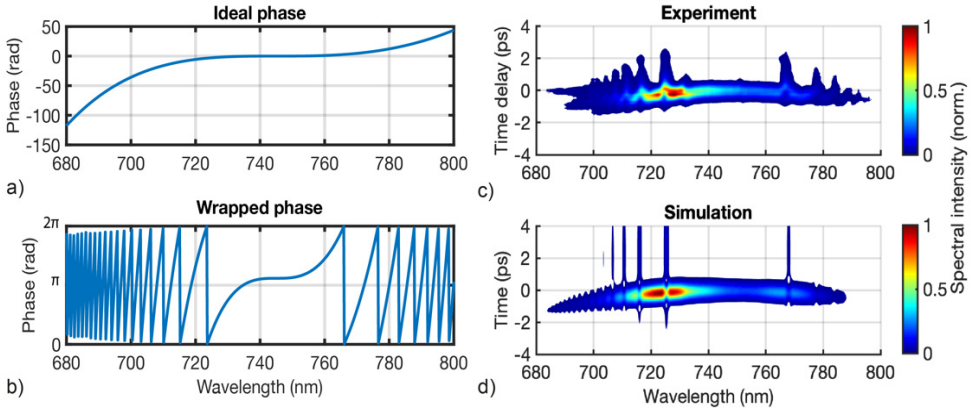

Fig. 3. (a) Ideal phase of −50000 fs^3 third-order dispersion (TOD) at a center wavelength of 745 nm. (b) Wrapped and smoothed phase from (a). (c) Non-collinear optical parametric amplifier (NOPA) amplified spectrum versus pump delay for a pulse with −50000 fs^3 TOD applied using the pulse shaper. For better contrast, only spectral amplitudes between 0.005 and 1 are plotted. (d) Simulated time-frequency analysis of a pulse on which the phase from (b) is applied.

Since we observe that the phase errors due to the pixel crosstalk mostly manifest ahead of the pulse, we chose to impose a negative GD offset of −2000 fs. In Fig. 4(a), we show the NOPA signal versus the pump delay when −2000 fs GD and −50000 fs^3 TOD was applied.

Optics EXPRESS

From the Fig. 4(a), we can identify 3 pulses: the zero-delayed pulse, which did not acquire the imposed phase; the pulse delayed by −2000 fs with the expected imposed phase and free from aberrations; and the replica advanced by 2000 fs due to phase smoothing errors with an opposite phase, i.e. positive TOD. The spectral amplitudes of the replica pulses depend strongly on how well the SLM phase response is calibrated. In this particular case, the SLM calibration is excellent over most of the bandwidth and hence only a very small part of the replica is visible. In Fig. 4(c), we contrast the acquired NOPA output spectrum for the case of 0 fs GD as it was shown in Fig. 3(c), and for the case when −2000 fs GD was imposed. Typically, in OPCPA systems the first nonlinear stage has a very high gain which naturally acts as an excellent temporal filter. By this temporal filtering, the effect of replica pulses is suppressed and a spectrally smooth amplification is achieved, as shown with the blue curve in Fig. 4(c). Finally, the seed pulse energy loss to replicas does not influence the overall system design, since the gain in the first amplification stage (which is usually very high gain for OPCPA systems) can be increased accordingly.

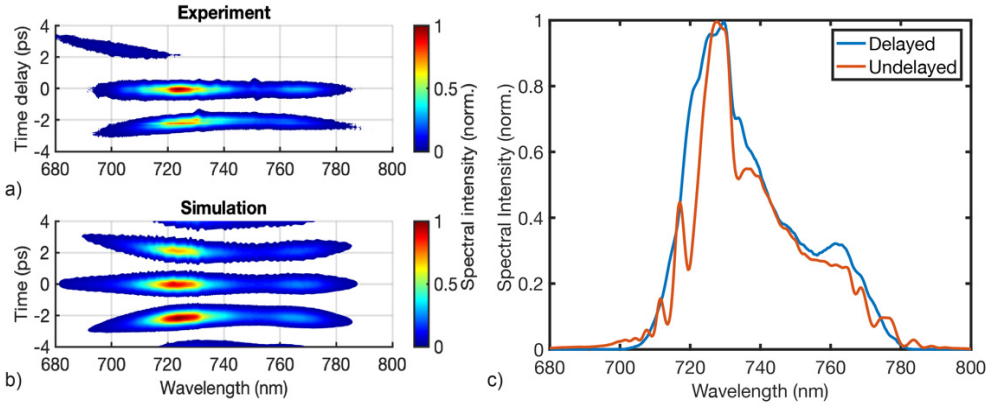

Fig. 4. (a) Non-collinear optical parametric amplifier (NOPA) amplified spectrum versus pump delay for a pulse with −2000 fs group-delay (GD) and −50000 fs^3 third-order dispersion (TOD) applied using the pulse shaper. For better contrast, only spectral amplitudes between 0.005 and 1 are plotted. (b) Simulated time-frequency analysis of a pulse on which a wrapped and smoothed phase of −2000 fs GD and −50000 fs^3 TOD was applied. (c) The measured NOPA output spectrum for the 0 fs GD case [as in Fig. 3 (c)], and for the −2000 fs GD case [shown in (a)].

To establish the utility of amplifying the pulse with a GD, we demonstrate that the amplified pulses can be compressed to the Fourier limit. By manually optimizing the phase $\varphi_{target}(\omega)$ at fixed GD offset of −2000 fs2, we could obtain a compressed pulse after amplification which we characterized with SH-FROG. The required phase $\varphi_{target}(\omega)$ varied by over 30 radians across the spectrum. Without the GD offset, this profile would cause 6 phase-wrapping points over the bandwidth, which in turn would distort the shaped waveform. In Fig. 5(a), we show the retrieved and measured spectra, as well as the remaining phase. Note that the phase over the energetic part of the spectrum is virtually flat, while at the wings of the spectrum the SH-FROG retrieval errors usually dominate. For comparison, the measured and retrieved traces are shown in Fig. 5(b). Furthermore, using a similar pulse shaper configuration, we have also demonstrated excellent pulse compression in the mid-infrared down-converted spectral range: our system yielded 1.7-cycle pulses at a center wavelength of 2500 nm with 12.6 W average power at 100 kHz, which is a record-short pulse duration for a >10 W mid-IR OPCPA [4].

Optics EXPRESS

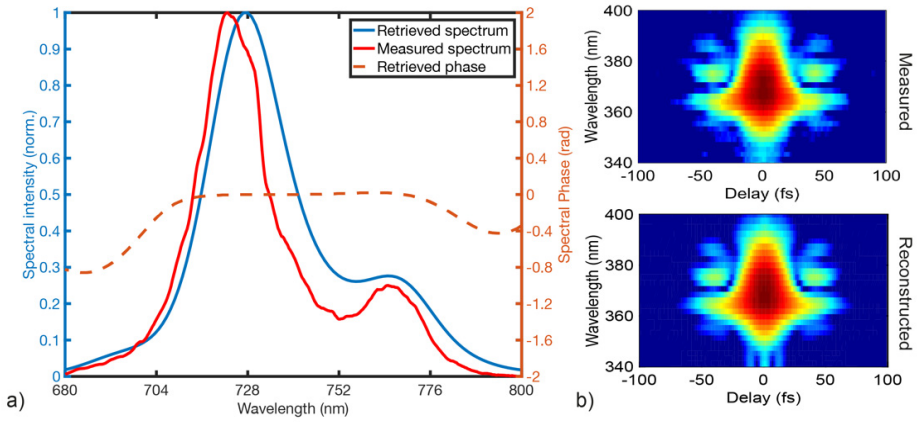

Fig. 5. (a) Retrieved spectrum and phase of the compressed pulse. The measured spectrum is overlaid for comparison. (b) Measured and reconstructed traces.

4. Spectral amplitude shaping

A powerful feature of using the pulse shaper with a large GD is the possibility to control the spectral intensity of the delayed components. This control can be achieved by scaling the amplitude of the wrapped phase profile. Intuitively, this approach can be understood by considering a spatial phase grating analogy. When a diffraction grating modulates the spatial phase by a modulation amplitude of 2π, then the diffraction to the 1st order is the most efficient. However, when the modulation amplitude is reduced, the optical power is redistributed into other diffraction orders. The same effectively happens in our pulse shaper in the time domain when a frequency grating is applied, as conceptually illustrated in Fig. 1.

In the pulse shaping case, when a large ideal phase profile is wrapped, it effectively acts like a phase grating applied in the frequency domain. Consider a large spectral phase $\varphi_{ideal}(\omega)$ applied on a pulse with spectral intensity distribution defined by $A(\omega)$. We apply an amplitude scaling factor ξ on a wrapped phase such that the modulation amplitude is scaled symmetrically over π:

$$\varphi_{wrapped} = \xi \cdot \mathrm{mod}(\varphi_{ideal}, 2\pi) - \pi(\xi - 1), \text{ for } \xi \in \Re[0,1] \tag{1}$$

It is important to stress that this is not equivalent to multiplying the unwrapped phase with the amplitude scaling factor since the modulo is not scale-invariant. As an example, consider applying a large GD which is phase-wrapped with a period of ω_p such that

$$\exp(i\varphi(\omega)) = \exp(i\frac{2\pi\xi\omega}{\omega_p} - i\pi(\xi - 1)), \text{ for } 0 \le \omega < \omega_p \tag{2}$$

This periodic phase function can be conveniently decomposed using Fourier series which leads to the output electric field:

$$E(\omega) = A(\omega)\sum_{n=-\infty}^{\infty} e^{-i\pi(n-1)}\,\mathrm{sinc}(\pi(\xi - n))\exp(i\frac{2\pi\omega}{\omega_p}n) \tag{3}$$

In this form, Eq. (3) can be interpreted as a frequency domain phase grating which leads to an infinite number of possible diffraction orders in the time domain separated by the applied GD. For the case when there is no phase wrapping amplitude modulation, i.e. $\xi = 1$, we find that all Fourier coefficients are zero, except the $n = 1$, which represents a linearly delayed pulse by $2\pi/\omega_p$. For the case when $\xi \neq 1$, all of the Fourier orders are contributing. If, in this case, we choose to time-filter only a chosen n^{th} diffraction order, we find that the

Optics EXPRESS

amplitude of the spectral component, ω, in the chosen diffraction order is defined by sinc(π(ξ-n)). It is worth noting that the applied phase is also scaled by the diffraction order n and the even terms acquire additional π phase shift. In contrast to the amplitude shaping described in [8], this scheme does not rely on a spatial diffraction-based filtering. The spectral components remain present in the beam, but are not delayed by the applied GD.

The crosstalk between the SLM pixels will lead to an effective smoothing of the wrapped-phase (as illustrated in Fig. 1), which in turn will reduce the grating modulation amplitude. Hence due to the crosstalk ξ will not be equal 1 and the modulator replicas will be present.

Because the GD is determined by the periodicity of the phase grating (i.e. GD = $2\pi/\omega_p$), the Eq. (3) can be extended to a more general phase which contains a large GD component. Any additional phase added will slightly change the local (i.e. in the vicinity of a spectral component ω) phase-wrapping periodicity. This will lead to an effectively different GD for this spectral component. Due to the varying period of the phase grating, this additional phase will be mapped to a GD spectrum.

Finally, because the phase grating has a spatial extent, it also acts as a weak spatial grating placed in the Fourier plane of the pulse shaper. This leads to a small, but noticeable lateral beam shift when a large GD is applied. This connection between delay and displacement (i.e. a form of spatiotemporal coupling) is a general property of pulse shapers based on SLMs [20]. This property can also lead to a spatial chirp if the applied additional phase significantly modifies the GD offset [21].

An SLM mask designed for a frequency-dependent amplitude shaping effect can be most easily evaluated numerically. We assume a compressed input pulse with a Gaussian spectral energy distribution. On this pulse, we apply a GD of –2000 fs and group delay dispersion (GDD) of 500 fs^2, and we additionally apply a flat-top amplitude mask of ξ = 0.5 for a part of the bandwidth as shown in Fig. 6(a). We model the pixel crosstalk by smoothing the wrapped phase using a moving average filter with a span of 8 pixels. Due to this pixel crosstalk and the amplitude mask, the modulator replicas appear in the time domain, as can be seen in Fig. 6(b). Furthermore, from the figure we can see that: (i) the undelayed pulse did not acquire any GDD; (ii) the the n = 1 diffraction order has acquired the designed phase and amplitude modulation; (iii) the n = 2 and n = –2 replicas acquired a phase which is twice larger than the designed phase, as expected from the Eq. (3). By temporally filtering the output, we can extract the spectral amplitude (Fig. 6(c)) of the delayed pulse, which indicates that the targeted spectral components were successfully suppressed.

Optics EXPRESS

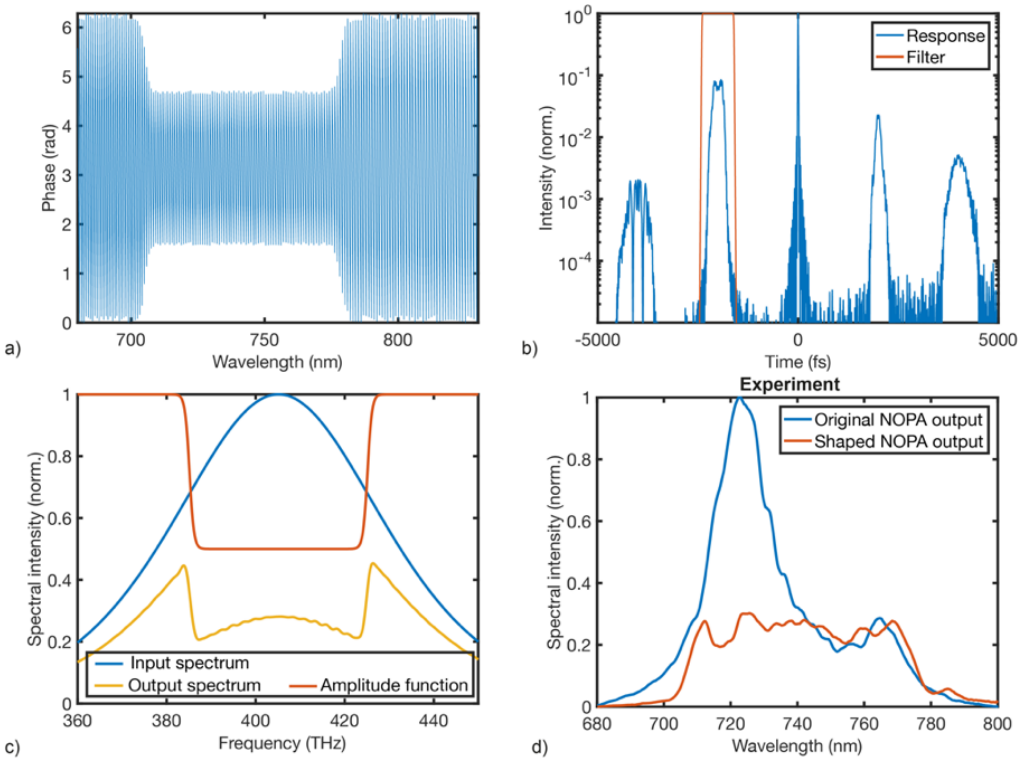

Fig. 6. (a) Simulation of an applied amplitude-scaled wrapped phase on a simulated Gaussian transform-limited pulse. The phase was −2000 fs group delay (GD) and 500 fs^2 group delay dispersion (GDD) for a central wavelength of 745 nm. (b) The time-domain representation of the simulated waveform in (a). The peak of the −2000-fs delayed pulse is suppressed as it would be expected for a linearly chirped and spectrally shaped pulse. (c) The spectral contents of the input and shaped pulses indicating spectral intensity shaping. (d) An experimental example of amplitude shaping where a nearly rectangular spectral intensity distribution was achieved after the non-collinear optical parametric amplifier (NOPA).

Next, we demonstrate this shaping experimentally by achieving a nearly flat-top amplified spectrum after the NOPA using a suitable phase profile at the SLM, as shown in Fig. 6(d). Note that because of the pixel crosstalk in the SLM and spectral gain coupling in the NOPA, an iterative algorithm would be required to achieve a perfectly flat-top shape.

In line with [7,12], we further demonstrate the amplitude and phase control by engineering a double-pulse waveform which is within the temporal gating window of our NOPA. We apply an additional GD of 400 fs for part of the bandwidth and, using amplitude filtering as shown in Fig. 7(a), we experimentally obtain the double-pulse profile at the output of the NOPA, as shown in Fig. 7(b). The relative amplitude of the pulses can be most easily controlled by adjusting the seed delay with respect to the pump.

Optics EXPRESS

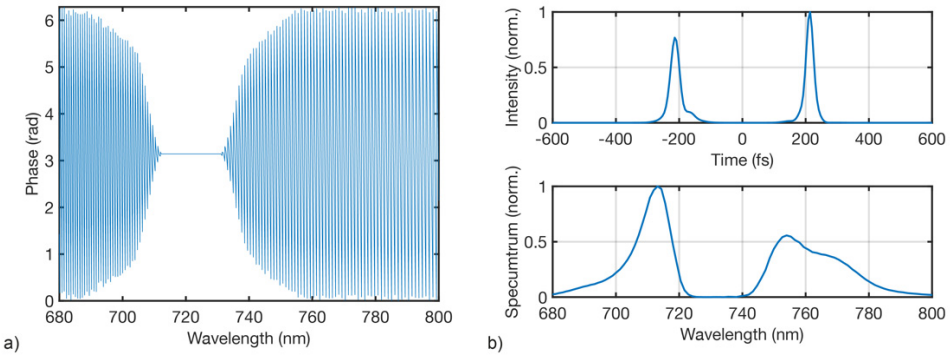

Fig. 7. (a) Experimentally applied amplitude control on the phase grating. The phase-grating contains the phase used to compress the pulse (as in Fig. 5.), a –2000 fs group delay (GD) over the complete bandwidth, as well as an additional 400 fs GD offset added for the spectral components with wavelength longer than 720 nm. (b) Reconstruction of the double-pulse from a second harmonic frequency resolved optical gating (SH-FROG) characterization.

5. Conclusion

We experimentally demonstrate a new SLM-based pulse shaping technique with which a large spectral phase can be imposed on the pulse without reducing the waveform quality. We achieve this operation by applying a large GD and time-gating the delayed pulse. Due to phase wrapping of this large GD, we create a phase grating in the frequency domain, which corresponds to a series of pulse replicas in time. We show that temporal filtering of a specific replica via time-gated amplification allows removing the temporal aberrations created by the pixelated nature of the SLM. Furthermore, we demonstrate that we can control the spectral amplitude of the shaped pulse by tuning the amplitude of the phase grating.

This is a powerful technique which allows shaping the amplitude and phase of ultrafast pulses by using only a 1D-SLM in conjunction with a time-gated amplifier. Implemented within the front-end of an OPCPA system, this pulse shaping technique can be used to compensate for a large dispersion without adding temporal aberrations to the pulses, hence avoiding the need for additional highly dispersive stretchers. Furthermore, the amplitude shaping function can be used to compensate for a spectrally dependent gain in broadband systems, enabling engineering of the most optimal waveforms for various applications. Particularly, gain narrowing in OPCPA systems can be mitigated and very high peak power waveforms can be achieved for strong-field applications, such as high-harmonic generation and attosecond science.

Funding

Swiss National Science Foundation (SNSF) projects (200021_159975 and 200020_172644).

References

1. A. M. Weiner, “Ultrafast optical pulse shaping: A tutorial review,” Opt. Commun. **284**(15), 3669–3692 (2011).
2. J. Rothhardt, S. Demmler, S. Hädrich, J. Limpert, and A. Tünnermann, “Octave-spanning OPCPA system delivering CEP-stable few-cycle pulses and 22 W of average power at 1 MHz repetition rate,” Opt. Express **20**(10), 10870–10878 (2012).
3. A. Harth, C. Guo, Y. Cheng, A. Losquin, M. Miranda, S. Mikaelsson, C. Heyl, O. Prochnow, J. Ahrens, U. Morgner, A. L. Huillier, and C. Arnold, “Compact 200 kHz HHG source driven by a few-cycle OPCPA,” J. Opt. **84**(7), 73103 (2016).
4. N. Bigler, J. Pupeikis, S. Hrisafov, L. Gallmann, C. R. Phillips, and U. Keller, “High-power OPCPA generating 1.7 cycle pulses at 2.5 μm,” Opt. Express **26**(20), 26750–26757 (2018).
5. J. Vaughan, T. Feurer, K. Stone, and K. Nelson, “Analysis of replica pulses in femtosecond pulse shaping with pixelated devices,” Opt. Express **14**(3), 1314–1328 (2006).
6. M. Wang, L. Zong, L. Mao, A. Marquez, Y. Ye, H. Zhao, and F. Vaquero Caballero, “LCoS SLM Study and Its Application in Wavelength Selective Switch,” Photonics **4**(4), 22 (2017).

Optics EXPRESS

7. J. C. Vaughan, T. Hornung, T. Feurer, and K. A. Nelson, "Diffraction-based femtosecond pulse shaping with a two-dimensional spatial light modulator," Opt. Lett. **30**(3), 323–325 (2005).
8. J. W. Wilson, P. Schlup, and R. A. Bartels, "Ultrafast phase and amplitude pulse shaping with a single, one-dimensional, high-resolution phase mask," Opt. Express **15**(14), 8979–8987 (2007).
9. P. Tournois, "Acousto-optic programmable dispersive filter for adaptive compensation of group delay time dispersion in laser systems," Opt. Commun. **140**(4–6), 245–249 (1997).
10. F. Verluise, V. Laude, Z. Cheng, C. Spielmann, and P. Tournois, "Amplitude and phase control of ultrashort pulses by use of an acousto-optic programmable dispersive filter: pulse compression and shaping," Opt. Lett. **25**(8), 575–577 (2000).
11. R. Budriūnas, T. Stanislauskas, J. Adamonis, A. Aleknavičius, G. Veitas, D. Gadonas, S. Balickas, A. Michailovas, and A. Varanavičius, "53 W average power CEP-stabilized OPCPA system delivering 5.5 TW few cycle pulses at 1 kHz repetition rate," Opt. Express **25**(5), 5797–5806 (2017).
12. P. Krogen, H. Suchowski, H. Liang, N. Flemens, K. Hong, F. X. Kärtner, and J. Moses, "Generation and multi-octave shaping of mid-infrared intense single-cycle pulses," Nat. Photonics **11**(4),222 (2017).
13. N. Thiré, R. Maksimenka, B. Kiss, C. Ferchaud, G. Gitzinger, T. Pinoteau, H. Jousselin, S. Jarosch, P. Bizouard, V. Di Pietro, E. Cormier, K. Osvay, and N. Forget, "Highly stable, 15 W, few-cycle, 65 mrad CEP-noise mid-IR OPCPA for statistical physics," Opt. Express **26**(21), 26907–26915 (2018).
14. A. Dubietis, G. Jonušauskas, and A. Piskarskas, "Powerful femtosecond pulse generation by chirped and stretched pulse parametric amplification in BBO crystal," Opt. Commun. **88**(4–6), 437–440 (1992).
15. S. Witte and K. S. E. Eikema, "Ultrafast optical parametric chirped-pulse amplification," IEEE J. Sel. Top. Quantum Electron. **18**(1), 296–307 (2012).
16. B. E. Schmidt, N. Thiré, M. Boivin, A. Laramée, F. Poitras, G. Lebrun, T. Ozaki, H. Ibrahim, and F. Légaré, "Frequency domain optical parametric amplification," Nat. Commun. **5**(1), 3643 (2014).
17. C. R. Phillips, B. W. Mayer, L. Gallmann, and U. Keller, "Frequency-domain nonlinear optics in two-dimensionally patterned quasi-phase-matching media," Opt. Express **24**(14), 15940–15953 (2016).
18. N. Bigler, J. Pupeikis, S. Hrisafov, L. Gallmann, C. R. Phillips, and U. Keller, "Decoupling phase-matching bandwidth and interaction geometry using non-collinear quasi-phase-matching gratings," Opt. Express **26**(5), 6036–6045 (2018).
19. D. J. Kane and R. Trebino, "Characterization of arbitrary femtosecond pulses using frequency-resolved optical gating," IEEE J. Quantum Electron. **29**(2), 571–579 (1993).
20. M. M. Wefers and K. A. Nelson, "Analysis of programmable ultrashort waveform generation using liquid-crystal spatial light modulators," J. Opt. Soc. Am. B **12**(7), 1343 (1995).
21. T. Tanabe, H. Tanabe, Y. Teramura, and F. Kannari, "Spatiotemporal measurements based on spatial spectral interferometry for ultrashort optical pulses shaped by a Fourier pulse shaper," J. Opt. Soc. Am. B **19**(11), 2795 (2002).

195.176.113.207 {ts '2020-04-07 10:43:04'}